高压物理学报
CHINESE JOURNAL OF HIGH PRESSURE PHYSICS

第 32 卷 第 1 期
2018 年 2 月

高 压 物 理 学 报
CHINESE JOURNAL OF HIGH PRESSURE PHYSICS

Vol. 32, No. 1
Feb., 2018

DOI: 10.11858/gywlxb.20170606

Structure and Properties of Novel Superhard C_5N: A First-Principles Study*

LI Zihe, LIU Chao, MA Mengdong, PAN Yilong, ZHAO Zhisheng, YU Dongli, HE Julong

(*State Key Laboratory of Metastable Materials Science and Technology, Yanshan University, Qinhuangdao* 066004, *China*)

Abstract: By using the developed particle swarm optimization algorithm on the crystal structural prediction, we proposed 6 novel carbon nitride phases with a 5 : 1 stoichiometry. Their structures, stability, mechanical and electronic properties were investigated by first-principle calculations with the density functional theory. Our calculations indicate that $P\bar{6}2m$-C_5N is energetically favorable in the 6 structures. Both elastic constants and phonon-dispersion calculations show that these structures remain mechanically and dynamically stable at 0 GPa. Electronic calculations indicate that $I4_1$-C_5N is metallic while the other 5 are semiconductive. The Vickers hardness shows that all the 6 structures are superhard materials except for $I4_1$-C_5N. Formation enthalpy calculations suggest that these 6 structures can be synthesized at attainable high pressures (19−83 GPa).

Keywords: carbon nitride; first-principle calculations; superhard; high shear modulus

CLC number: O481.1; O482.1 **Document code**: A

Superhard materials (Vickers hardness $H_v \geqslant 40$ GPa) are of fundamental interest and practical importance due to their outstanding mechanical and thermal properties, such as excellent hardness, high melting point, and wear resistance. Diamond and cubic-BN (c-BN) are two types of typical superhard materials that have been widely used in industry because of the aforementioned superior properties. However, in the past few decades, the search for new superhard materials has continued. In this context, carbon nitride has become a primary candidate for low-compressibility or superhard materials due to its relatively short bond length and low bond ionicity[1]. Since the pioneering work of Liu and Cohen[2-3] that predicted hexagonal β-C_3N_4 with extraordinary hardness, considerable efforts have been devoted theoretically[4-14] and experimentally[15-24] to searching new stoichiometric carbon nitride materials with novel properties. On the theoretical side, several approaches have been applied to predict and design new superhard carbon nitrides with different stoichiometries, such as $Pnnm$-CN, $P4_2/m$-CN, α-C_3N_2, and bct-CN_2. On the experimental side, melamine, cyanamide, and other related triazine-based compounds can be used as precursors to synthesize α-, β-, and mainly g-C_3N_4 through different mechanochemical techniques in the form of thin films and nanocrystals. However, these structures have been unverified because of the limited quantity and heterogeneity of the samples, thereby resulting in exten-

* **Received date**: 2017-06-29; **Revised date**: 2017-07-08

Foundation item: National Natural Science Foundation of China (51421091, 51332005)

Biography: LI Zihe (1990—), male, doctoral student, major in research of metastable materials. E-mail: lizihelegend@163.com

Corresponding author: HE Julong (1958—), male, doctor, professor, major in research of metastable materials. E-mail: hjl@ysu.edu.cn

© 2018 Institute of Fluid Physics, China Academy of Engineering Physics

sive debates. Other structure phases of carbon nitride may exist besides C_3N_4. Recently, Stavrou et al.[25] synthesized *Pnnm*-CN using single-crystal graphite and high-pressure gas-loaded N_2 in a standard laser heated (LH) diamond anvil cell (DAC) configuration. This research achievement verifies the aforementioned assumption. Therefore, with the theoretical calculations guiding the research, other carbon nitrides with different stoichiometric measurements should be designed and calculated in the future.

1 Method

The crystal structure search is based on the global minimization of free energy surfaces merging *ab initio* total energy calculations through the particle swarm optimization (PSO) technique as implemented in the CALYPSO code[26]. First-principle calculations were performed using the CASTEP[27] code based on the density functional theory[28-29]. The exchange and correlation effects were described by the generalized gradient approximation-Perdew-Burke-Ernzerh (GGA-PBE) exchange-correlation functional[30]. Ultrasoft pseudopotentials were expanded using a plane-wave basis set with a cutoff energy of 500 eV, and a k-point spacing ($2\pi\times0.4\ \mathrm{nm}^{-1}$) was assigned to generate Monkhorst-Pack k-point grids for Brillouin zone sampling[31]. Structural optimization using the BFGS minimization method was performed until the energy change of each atom was less than 5×10^{-6} eV, the forces on atoms were less than $0.1\ \mathrm{eV\cdot nm^{-1}}$, and all the stress components were less than 0.02 GPa[32]. The phonon modes of the equilibrium crystal structure obtained after structural relaxation were calculated using the finite displacement theory[33]. For the calculated phonon dispersion in reciprocal space, the high symmetry point coordinates were G (0,0,0), A (0,0,0.5), H (−0.33,0.67,0.50), K (−0.33, 0.67,0), M (0,0.5,0), and L (0,0.5,0.5). The polycrystalline bulk modulus, shear modulus, Young's modulus, and Poisson's ratio were estimated using the Voigt-Reuss-Hill approximation[34].

2 Results and Discussions

2.1 Crystal Structure

Through the CALYPSO code, crystal structure searches were performed with a cell size of up to 48 atoms (40 C atoms and 8 N atoms) within a pressure range of 0−70 GPa. Analysis of the predicted structures gives us a shortlist of candidate structures with space groups $P\bar{6}2m$ (2 formula units per cell), $I4_1$ (4 formula units per cell), *Pbcn* (8 formula units per cell), $P6_3cm$ (8 formula units per cell), $P2_12_12_1$ (8 formula units per cell) and $Pna2_1$ (8 formula units per cell), respectively, as shown in Fig. 1. In these novel structures, $I4_1$-C_5N and $P6_3cm$-C_5N are sp^2-sp^3 hybridized while the other 4 are all sp^3 hybridized phases. The N atoms and the 3 bonded C atoms are almost coplanar in the $P\bar{6}2m$-C_5N, $I4_1$-C_5N, *Pbcn*-C_5N and $P6_3cm$-C_5N structures, while they form a tetrahedron in the $Pna2_1$-C_5N. Furthermore, in the $P2_12_12_1$-C_5N structure, these 2 kinds of N atoms both exist. The optimized lattice parameters, atom positions, space groups, densities and cell volumes of the 6 types of C_5N are obtained and listed in Table 1.

2.2 Stability Analysis

To explore the thermodynamic stability for further experimental synthesis, the formation enthalpy of the 6 novel C_5N structures with respect to the separate phases is quantified by $\Delta H_f = E_{C_5N} - 5E_C - (1/2)E_{N_2}$, where E_{C_5N} is the ground state enthalpy of the new C_5N phase, E_C is the energy of C atom obtained from graphite, and E_{N_2} is the total energy of the stable molecular α phase of nitrogen reported earlier[35]. The calculated formation enthalpy of these C_5N structures as functions of pressure is shown in Fig. 2.

Table 1　Structure parameters of the newly predicted C_5N

Phase	Crystal system	Space group	Atoms positions	Lattice parameters/nm	Density/(g·cm^{-3})	Cell volume/nm^3
$P\bar{6}2m$-C_5N	Hexagonal	$P\bar{6}2m$	C:6*i* (0.668 6, 0, 0.685 1) C:4*h* (0.333 3, 0.666 7, 0.184 6) N:2*e* (0, 0, 0.252 0)	*a*=0.426 10 *c*=0.449 04	3.483 66	0.070 605 6
$I4_1$-C_5N	Tetragonal	$I4_1$	C:8*b* (1.392 2, 0.304 7, 0.221 3) C:8*b* (0.888 8, 0.302 5, 0.565 1) C:4*a* (0.500 0, −0.500 0, 0.664 9) N:4*a* (0.500 0, −0.500 0, 0.371 7)	*a*=0.565 54 *c*=0.461 99	3.329 25	0.147 761
Pbcn-C_5N	Orthorhombic	*Pbcn*	C:8*d* (0.839 4, 1.185 9, 0.665 3) C:8*d* (0.944 3, 0.510 5, 1.378 0) C:8*d* (0.727 2, 1.419 3, 1.396 7) C:8*d* (1.416 5, 1.445 1, 0.543 3) C:4*c* (0.500 0, 1.349 1, 0.750 0) C:4*c* (0.500 0, 0.812 5, 0.750 0) N:8*d* (1.315 9, 0.707 9, 1.403 3)	*a*=0.692 19 *b*=0.759 85 *c*=0.552 51	3.385 59	0.290 603
$P6_3cm$-C_5N	Hexagonal	$P6_3cm$	C:12*d* (0.154 9, 0.410 3, 0.866 7) C:12*d* (0.409 9, 0.154 2, 0.693 1) C:6*c* (0.782 2, 0, 0.648 6) C:4*b* (0.333 3, 0.666 7, 0.124 7) C:4*b* (0.333 3, 0.666 7, 0.941 3) C:2*a* (0, 0, 0.414 3) N:6*c* (0.784 7, 0, 0.910 1) N:2*a* (0, 0, 0.151 9)	*a*=0.615 46 *c*=0.943 32	3.179 45	0.309 444
$P2_12_12_1$-C_5N	Orthorhombic	$P2_12_12_1$	C:4*a* (−0.466 0, 0.364 8, 0.025 1) C:4*a* (−0.035 6, 0.414 0, 0.784 6) C:4*a* (0.408 2, 0.755 3, 0.494 3) C:4*a* (−0.302 6, 0.231 6, 0.496 5) C:4*a* (−0.341 4, 0.702 3, 0.989 9) C:4*a* (0.432 1, 0.397 5, 0.519 8) C:4*a* (−0.445 0, 0.692 8, 0.481 2) C:4*a* (0.124 6, 0.438 9, 0.522 9) C:4*a* (0.313 1, 0.924 8, 0.470 3) C:4*a* (−0.072 2, 0.990 7, 0.477 8) N:4*a* (−0.253 6, 0.868 1, 0.988 5) N:4*a* (−0.286 0, 0.600 1, 0.055 7)	*a*=0.804 49 *b*=1.408 89 *c*=0.256 59	3.383 0	0.290 827
$Pna2_1$-C_5N	Orthorhombic	$Pna2_1$	C:4*a* (0.626 2, 0.290 9, 0.796 6) C:4*a* (0.666 9, 0.499 9, 0.848 8) C:4*a* (0.445 7, 0.119 1, 0.129 6) C:4*a* (0.351 3, 0.008 5, 0.110 2) C:4*a* (0.441 2, 0.811 5, 0.859 2) C:4*a* (0.103 0, 0.160 9, 0.066 6) C:4*a* (0.975 7, 0.200 5, 0.331 8) C:4*a* (0.261 7, 0.152 7, 0.541 9) C:4*a* (0.748 6, 0.623 5, 0.458 7) C:4*a* (0.311 9, 0.039 9, 0.607 6) N:4*a* (0.322 5, 0.479 6, 0.860 4) N:4*a* (0.771 2, 0.200 0, 0.776 8)	*a*=0.402 99 *b*=1.402 05 *c*=0.516 40	3.372 0	0.291 776

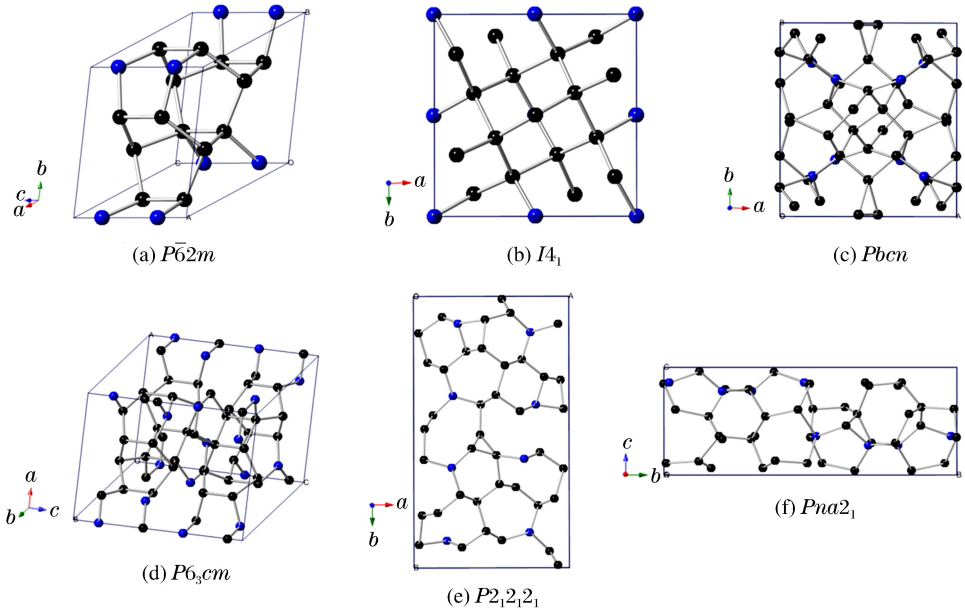

Fig. 1　Predicted structure graphs of C_5N (The spheres in color black and blue represent C and N atoms, respectively.)

From Fig. 2, the formation enthalpies suggest that these C_5N phase is metastable at 0 GPa because of its positive value, which is similar to that of diamond and c-BN. Meanwhile, as the pressure rises from 19 GPa to 83 GPa, all these 6 phases gradually become thermodynamically stable. Moreover, the use of high temperature is a classical way to improve both the diffusion processes and the reactivity of precursors for the material synthesis of bulk forms or thin films. That is, if we use graphite and nitrogen as precursors for condensed carbon nitrides at high pressure, then these C_5N phases may be synthesized at readily attainable pressures and temperatures. Furthermore, our phonon calculations have verified that these 6 C_5N is dynamically stable as evidenced by the absence of any imaginary frequency in the whole Brillouin zone at ambient pressure (see Fig. 3).

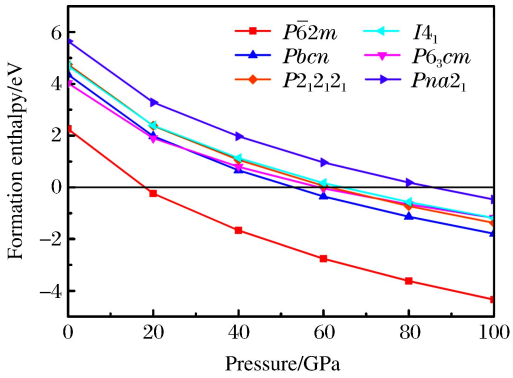

Fig. 2　Formation enthalpy of the newly predicted C_5N phases relative to graphite and nitrogen as a function of pressure

To evaluate the mechanical stability of a crystal structure, the elastic constants of a crystal should satisfy the generalized elastic stability criteria. For a hexagonal crystal, 5 independent elastic constants, namely, C_{11}, C_{33}, C_{44}, C_{12}, and C_{13}, should obey the following generalized Born mechanical stability criteria[35]: $C_{44}>0$, $C_{11}>|C_{12}|$, and $(C_{11}+2C_{12})C_{33}>2C_{13}^2$. For a tetragonal crystal, there are 6 independent elastic constants, namely, C_{11}, C_{33}, C_{44}, C_{66}, C_{12}, and C_{13}, and the corresponding mechanical stability criterion is given by: $C_{ij}>0$ $(i=j=1-6)$, $C_{11}-C_{12}>0$, $C_{11}+C_{33}-2C_{13}>0$, $2(C_{11}+C_{12})+C_{33}+4C_{13}>0$. For an orthorhombic crystal, there are 9 independent elastic constants, namely, C_{11}, C_{22}, C_{33}, C_{44}, C_{55}, C_{66}, C_{12}, C_{13} and C_{23}, and the corresponding mechanical stability criterion is as follow: $C_{ij}>0$

$(i=j=1\text{-}6)$, $C_{11}+C_{22}+C_{33}+2(C_{12}+C_{13}+C_{23})>0$, $C_{11}+C_{22}-2C_{12}>0$, $C_{11}+C_{33}-2C_{13}>0$, $C_{22}+C_{33}-2C_{23}>0$. The calculated elastic constant values of C_5N phases by the strain-stress method are listed in Table 2. According to the above criteria, the calculation results indicate that these novel structures are all mechanically stable under ambient pressure.

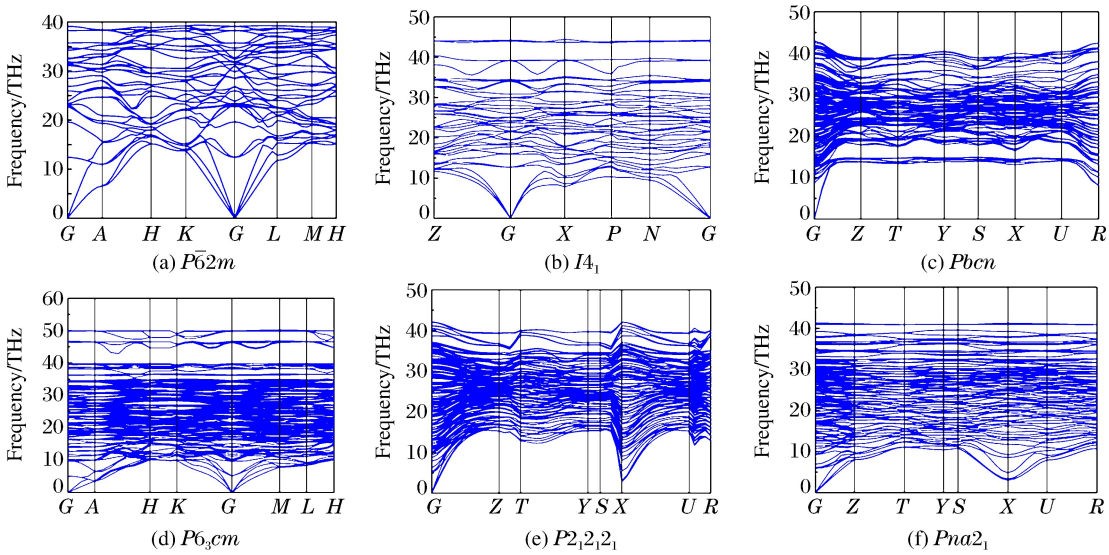

Fig. 3　Phonon dispersion spectrum at 0 GPa

Table 2　Calculated independent elastic constants C_{ij} of the newly predicted C_5N

Phase	C_{11}/GPa	C_{22}/GPa	C_{33}/GPa	C_{44}/GPa	C_{55}/GPa	C_{66}/GPa	C_{12}/GPa	C_{13}/GPa	C_{15}/GPa	C_{23}/GPa	C_{25}/GPa
$P\bar{6}2m$-C_5N	1 194		930	252			113	18			
$I4_1$-C_5N	649		931	244		247	244	75			
$Pbcn$-C_5N	762	663	822	382	360	364	190	83	165		
$P6_3cm$-C_5N	873		490	192			170	35			
$P2_12_12_1$-C_5N	902	847	893	299	341	347	120	93	40	902	847
$Pna2_1$-C_5N	891	659	736	289	372	324	86	153	149	891	659

2.3　Properties

Based on the Voigt-Reuss-Hill approximation, bulk modulus (B), shear modulus (G), Young's modulus (E) and Poisson's ratio (σ) can be obtained from the calculated elastic constants. The calculated B, G, E and σ of the newly predicted C_5N are listed in Table 3. Bulk modulus is a measure of the resistance against volume change imposed by the applied pressure, while shear modulus represents the resistance to the shear deformation against external forces, which indicates the resistance to the change in the bond angle. The hardness is deduced from the size of the indentation after deformation. A superhard material typically requires a high bulk modulus to support the volume decrease created by the applied pressure and a high shear modulus so that the material will not deform in a direction different from that of the applied load. From Table 3, it is obvious that both B and G of $P\bar{6}2m$-C_5N are the largest among the 6 new structures, indicating it can withstand stronger compression and higher shear stress than the other structures.

The relative directionality of covalent bonds of materials also has an important effect on their hardness and mechanical properties, which can be determined by the G/B ratio[36]. Table 3 shows that the G/B ratio of $P2_12_12_1$-C_5N (1.014) is higher than that of the other 5 C_5N phases, thereby suggesting the stronger directional bonding feature of $P2_12_12_1$-C_5N. The relative orientation of material bonding also has an important effect on their hardness. Young's modulus (E) is defined as the ratio between stress and strain and is used to provide a measure of stiffness of the solid, i. e., the larger the value of E, the stiffer the material is. Poisson's ratio (σ) quantifies the stability of the crystal against shear. Except for $I4_1$-C_5N, the fairly large value of E and small Poisson's ratio indicate that the other 5 C_5N phases are rather stiff and relatively stable against shear. Thus, the preceding results reveal that these new C_5N phases are potential candidates for superhard materials and this will be confirmed by our following calculations of the Vickers hardness.

Table 3　Calculated bulk modulus B, shear modulus G, Young's modulus E and Vickers hardness H_v of the newly predicted C_5N (Also shown are G/B ratio and Poisson's ratio σ)

Phase	B/GPa	G/GPa	E/GPa	σ	G/B	H_v/GPa
$P\bar{6}2m$-C_5N	397	394	888	0.127	0.992	62.5
$I4_1$-C_5N	335	238	577	0.213	0.711	30.0
$Pbcn$-C_5N	347	338	765	0.133	0.973	55.0
$P6_3cm$-C_5N	286	267	611	0.144	0.934	44.5
$P2_12_12_1$-C_5N	349	354	794	0.121	1.014	59.6
$Pna2_1$-C_5N	338	321	731	0.139	0.949	51.6

The electronic structure determines the fundamental physical and chemical properties of materials. The calculated electronic band structure of the new predicted C_5N phases at 0 GPa are presented in Fig. 4. From Fig. 4, we can find that $I4_1$-C_5N are metallic, $Pbcn$-C_5N and $Pna2_1$-C_5N are direct-bandgap semiconductors while $P\bar{6}2m$-C_5N, $P6_3cm$-C_5N and $P2_12_12_1$-C_5N are indirect-bandgap semiconductors. All these 5 semiconductors are narrow bandgap semiconductors and their bandgaps are 1.131, 0.971, 2.312, 0.796 and 1.088 eV, respectively. The narrow bandgap feature suggests that they

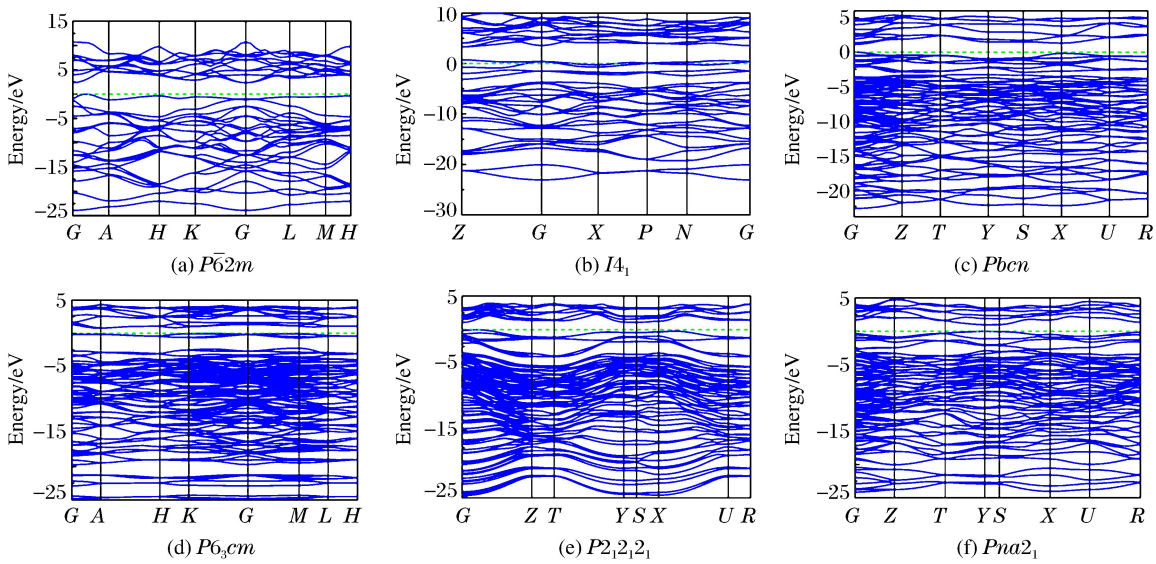

Fig. 4　Electronic band structures of newly predicted C_5N at 0 GPa

may be used as photocatalyst. In addition, the direct bandgap feature indicates *Pbcn*-C_5N and *Pna*2_1-C_5N are promising materials for the solar cell or photography industry.

In order to figure out the theoretical Vickers hardness of the new C_5N structures, we employed the macroscopic hardness model proposed by Chen *et al*.[37] and revised by Tian *et al*.[38]. The formula is $H_v(\mathrm{GPa})=0.92k^{1.137}G^{0.708}$, where k is the Pugh modulus ratio and equal to G/B. The results are shown in Table 3. We can find that these new compounds are superhard materials except for $I4_1$-C_5N and the hardness of $P\bar{6}2m$-C_5N and $P2_12_12_1$-C_5N are even close to that of c-BN.

3 Conclusions

In summary, using the developed PSO technique on the crystal structure prediction, we predicted 6 types of C_5N structures, and systematically investigated their geometry structures, stability, electronic and mechanical properties by first-principle calculations based on the density functional theory. All these new phases are metastable at ambient pressure but become energetically more stable than graphite and N_2 under high pressures (19－83 GPa). In addition, they are proved to be mechanically and dynamically stable at ambient pressure by computing their elastic constants and phonon dispersions. Furthermore, except for $I4_1$-C_5N, the other 5 phases are superhard semiconductors as well. The present work has great implications for designing and researching novel superhard materials.

References:

[1] LÉGER J-M, HAINES J. The search for superhard materials [J]. Endeavour, 1997, 21(3): 121-124.

[2] LIU A Y, COHEN M L. Prediction of new low compressibility solids [J]. Science, 1989, 245(4920): 841-842.

[3] LIU A Y, COHEN M L. Structural properties and electronic structure of low-compressibility materials: β-Si_3N_4 and hypothetical β-C_3N_4 [J]. Physical Review B, 1990, 41(15): 10727-10734.

[4] CÔTÉAND M, COHEN M L. Carbon nitride compounds with 1∶1 stoichiometry [J]. Physical Review B, 1997, 55(9): 5684.

[5] HALES J, BARNARD A S. Thermodynamic stability and electronic structure of small carbon nitride nanotubes [J]. Journal of Physics: Condensed Matter, 2009, 21(14): 144203.

[6] KIM E, CHEN C, KÖHLER T, et al. Tetragonal crystalline carbon nitrides: theoretical predictions [J]. Physical Review Letters, 2001, 86(4): 652-655.

[7] KIM E, CHEN C. Stability of tetragonal crystalline carbon nitrides: the nitrogen content dependence [J]. Physics Letters A, 2001, 282(6): 415-420.

[8] HART J N, CLAEYSSENS F, ALLAN N L, et al. Carbon nitride: *ab initio* investigation of carbon-rich phases [J]. Physical Review B, 2009, 80(17): 174111.

[9] SANDRÉ É, PICKARD C J, COLLIEX C. What are the possible structures for CN_x compounds? The example of C_3N [J]. Chemical Physics Letters, 2000, 325(1/2/3): 53-60.

[10] TIAN F, WANG J, HE Z, et al. Superhard semiconducting C_3N_2 compounds predicted via first-principles calculations [J]. Physical Review B, 2008, 78(23): 235431.

[11] WANG X. Polymorphic phases of sp^3-hybridized superhard CN [J]. The Journal of Chemical Physics, 2012, 137(18): 184506.

[12] ZHANG M, WEI Q, YAN H, et al. A novel superhard tetragonal carbon mononitride [J]. The Journal of Physical Chemistry C, 2014, 118(6): 3202-3208.

[13] LI Q, LIU H, ZHOU D, et al. A novel low compressible and superhard carbon nitride: body-centered tetragonal CN_2 [J]. Physical Chemistry Chemical Physics, 2012, 14(37): 13081-13087.

[14] XU Y, GAO S P. Band gap of C_3N_4 in the GW approximation [J]. International Journal of Hydrogen Energy, 2012, 37(15): 11072-11080.

[15] GUO L P, CHEN Y, WANG E G, et al. Identification of a new tetragonal C-N phase [J]. Journal of Crystal Growth, 1997, 178(4): 639-644.

[16] SEKINE T, KANDA H, BANDO Y, et al. A graphitic carbon nitride [J]. Journal of Materials Science Letters, 1990, 9(12): 1376-1378.

[17] STEVENS A J, KOGA T, AGEE C B, et al. Stability of carbon nitride materials at high pressure and temperature [J]. Journal of the American Chemical Society, 1996, 118(44): 10900-10901.

[18] STEVENS A J, AGEE C B, LIEBER C M. High-pressure chemistry of carbon nitride materials [J/OL]. MRS Online Proceedings Library, 1997, 499: 309(2011-02-01)[2017-06-29]. https://doi.org/10.1557/PROC-499-309.

[19] CHEN Y A, GUO L, WANG E G. Alpha beta experimental evidence for alpha- and beta-phases of pure crystalline C_3N_4 in films deposited on nickel substrates [J]. Philosophical Magazine Letters, 1997, 75(3): 155-162.

[20] NIU C, LU Y Z, LIEBER C M. Experimental realization of the covalent solid carbon nitride [J]. Science, 1993, 261(5119): 334-337.

[21] YU K M, COHEN M L, HALLER E E, et al. Observation of crystalline C_3N_4 [J]. Physical Review B, 1994, 49(7): 5034-5037.

[22] YIN L W, LI M S, LIU Y X, et al. Synthesis of beta carbon nitride nanosized crystal through mechanochemical reaction [J]. Journal of Physics: Condensed Matter, 2003, 15(2): 309-314.

[23] GUO Q, XIE Y, WANG X, et al. Characterization of well-crystallized graphitic carbon nitride nanocrystallites via a benzene-thermal route at low temperatures [J]. Chemical Physics Letters, 2003, 380(1/2): 84-87.

[24] JÜRGENS B, IRRAN E, SENKER J, et al. Melem (2,5,8-triamino-tri-*s*-triazine), an important intermediate during condensation of melamine rings to graphitic carbon nitride: synthesis, structure determination by X-ray powder diffractometry, solid-state NMR, and theoretical studies [J]. Journal of the American Chemical Society, 2003, 125(34): 10288-10300.

[25] STAVROU E, LOBANOV S, DONG H, et al. Synthesis of ultra-incompressible sp^3-hybridized carbon nitride with 1∶1 stoichiometry [J]. Chemistry of Materials, 2016, 28(19): 6925-6933.

[26] WANG Y, LÜ J, ZHU L, et al. Crystal structure prediction via particle-swarm optimization [J]. Physical Review B, 2010, 82(9): 094116.

[27] SEGALL M D, PHILIP J D L, PROBERT M J, et al. First-principles simulation: ideas, illustrations and the CASTEP code [J]. Journal of Physics: Condensed Matter, 2002, 14(11): 2717-2744.

[28] KOHN W, SHAM L J. Self-consistent equations including exchange and correlation effects [J]. Physical Review A, 1965, 140(4): 1133-1138.

[29] HOHENBERG P, KOHN W. Inhomogeneous electron gas [J]. Physical Review B, 1964, 136(3): 864-871.

[30] JONES R O, GUNNARSSON O. The density functional formalism, its applications and prospects [J]. Reviews of Modern Physics, 1989, 61(3): 689-746.

[31] MONKHORST H J, PACK J D. Special points for Brillouin-zone integrations [J]. Physical Review B, 1976, 13(12): 5188-5192.

[32] FISCHER T H, ALMLOF J. General methods for geometry and wave function optimization [J]. The Journal of Physical Chemistry, 1992, 96(24): 9768-9774.

[33] CLARK S J, SEGALL M D, PICKARD C J, et al. First principles methods using CASTEP [J]. Zeitschrift für Kristallographie-Crystalline Materials, 2005, 220(5/6): 567-570.

[34] HILL R. The elastic behaviour of a crystalline aggregate [J]. Proceedings of the Physical Society: Section A, 1952, 65(5): 349.

[35] VENABLES J A, ENGLISH C A. Electron diffraction and the structure of α-N_2 [J]. Acta Crystallographica Section B: Structural Science, Crystal Engineering and Materials, 1974, 30: 929-935.

[36] WU Z J, ZHAO E J, XIANG H P, et al. Crystal structures and elastic properties of superhard IrN_2 and IrN_3 from first principles [J]. Physical Review B, 2007, 76(5): 054115.

[37] CHEN X Q, NIU H, LI D, et al. Modeling hardness of polycrystalline materials and bulk metallic glasses [J]. Intermetallics, 2011, 19(9): 1275-1281.

[38] TIAN Y, XU B, ZHAO Z. Microscopic theory of hardness and design of novel superhard crystals [J]. International Journal of Refractory Metals and Hard Materials, 2012, 33: 93-106.

新型超硬 C_5N 晶体结构及性能的第一性原理研究

李子鹤，刘　超，马梦东，潘益龙，赵智胜，于栋利，何巨龙

（燕山大学亚稳材料制备技术与科学国家重点实验室，河北 秦皇岛　066004）

摘要：通过使用在晶体结构预测方面成熟的粒子群优化算法，提出了 6 种化学计量比为 5∶1 的氮化碳新相。采用基于密度泛函理论的第一性原理计算研究它们的结构、稳定性、机械性能和电子性质。计算结果表明，在提出的 6 种结构中，$P\bar{6}2m$-C_5N 是能量最稳定的。弹性常数和声子谱计算表明，这些结构在 0 GPa 时是机械稳定和动力学稳定的。电子计算显示，$I4_1$-C_5N 是金属性的，而其他 5 种结构是半导体。维氏硬度计算表明，除 $I4_1$-C_5N 外，其余氮化碳都为超硬材料。通过形成焓计算，分析认为这 6 种结构能在目前实验所能达到的高压下合成（19～83 GPa）。

关键词：氮化碳；第一性原理计算；超硬；高剪切强度

中图分类号：O481.1；O482.1　　**文献标识码**：A